OPTIMAL IMPEDANCE CONTROL OF A 3 DOF ROBOT

Abdullah ERDEMİR

MPG Machinery Production Group Inc. Co.

ORCID NO: 0000-0002-7267-3111

Mete KALYONCU

Prof. Dr., Konya Technical University

ORCID ID: 0000-0002-2214-7631

ABSTRACT

This study aims to optimize the impedance control of a 3 degree-of-freedom (DOF) robot in various industrial applications, such as pushing, polishing, cleaning, and grinding. In these applications, the robot manipulator needs to interact with the environment to achieve the desired task, making it imperative to control the interaction between the robot and the environment. The impedance controller is an effective approach that regulates the dynamic relationship between the robot and the environment, which is crucial for performing these tasks accurately and efficiently. Unlike force/position hybrid controllers that have separate subspaces for force and position control, the proposed impedance controller aims to regulate the relationship between the force and the position of the end effector in contact with the environment. This approach ensures that the robot manipulator endpoint follows both the desired force profile and the desired position accurately. Additionally, the proposed method allows for planning a virtual trajectory to obtain a desired force profile when the environment has a rigid structure with known properties. To optimize the proposed impedance controller, the Bees Algorithm was used. The numerical application results demonstrate that the optimized impedance controller allows the robot manipulator endpoint to follow both the desired force profile and the desired position accurately, providing a practical solution for controlling the interaction between the robot manipulator and the environment in various industrial applications. The significance of this study lies in its potential to improve the performance of industrial robots in applications that require interaction with the environment. By using an optimized impedance controller, the robot can perform its task accurately and efficiently, reducing the risk of errors and improving productivity.

Keywords: Impedance control, 3 DOF robot, robot-environment interaction, The Bees Algorithm.

1. INTRODUCTION

Industrial robots are widely used in various manufacturing processes to automate tasks and improve productivity. In many industrial applications, the robot manipulator needs to interact with the environment to achieve the desired task, such as pushing, polishing, cleaning, and grinding. However, controlling the interaction between the robot and the environment can be challenging, as the robot needs to regulate the dynamic relationship between the force and position of the end effector in contact with the environment [1, 2].

One effective approach to regulate this dynamic relationship is through impedance control.

Unlike force/position hybrid controllers that have separate subspaces for force and position control, impedance controllers aim to regulate the relationship between the force and the position of the end effector in contact with the environment [3-5]. This approach ensures that the robot manipulator endpoint follows both the desired force profile and the desired position accurately [6, 7]. Impedance control has been widely studied and applied in various industrial applications, such as assembly, welding, and machining. In impedance control, the trajectory function of the robot's end effector is an essential factor that affects the dynamic relationship between the robot and the environment [8].

Optimization algorithms are a fundamental tool used in many scientific fields to solve complex problems. Two categories of optimization algorithms exist: global optimization algorithms and local search algorithms [9]. Global optimization algorithms, such as Genetic Algorithm [10, 11], Particle Swarm Optimization [12], and The Bees Algorithm [13-15], are designed to explore the entire solution space to find the global optimum. In contrast, local search algorithms such as Hooke-Jeeves [16] and Newton Raphson [17] focus on exploring local regions of the solution space to identify the optimum. While global optimization algorithms are generally more effective in finding the global optimum, local search algorithms can be faster and more efficient in identifying the optimum in small or restricted regions of the solution space. The choice of which optimization algorithm to use depends on the nature of the optimization problem and the characteristics of the solution space [18].

The focus of this study is to optimize the impedance control parameters of a 3 degree-of-freedom (DOF) robot in order to accurately control its movements and applying force on stations in industrial applications. The primary objective is to determine the optimal impedance control parameters that generate an accurate force profile. To achieve this objective, the Bees Algorithm was employed to optimize the impedance control parameters and minimize the relative distance and force errors as objective function [6, 19]. By using the optimized impedance controller, the robot can perform its task accurately and efficiently, reducing the risk of errors and improving productivity in various industrial applications.

2. MATHEMATICAL MODEL

The focus of this research is the 3 degree-of-freedom (DOF) manipulator, which consists of three joints. The manipulator's physical configuration is composed of three links with individual masses denoted as m_1, m_2, and m_3, as illustrated in Figure 1.

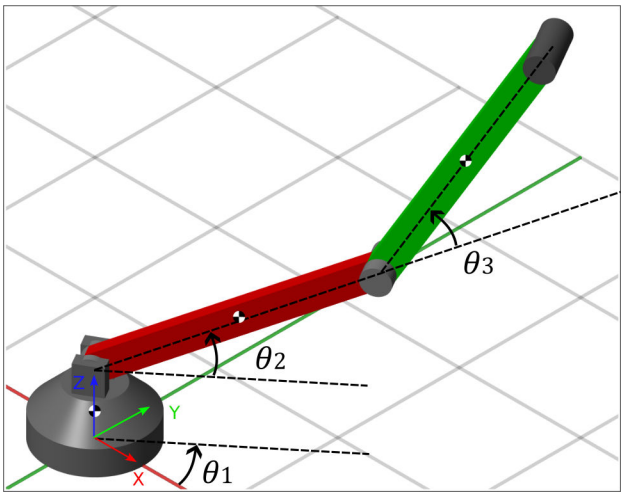

Figure 1. 3 dof robotic system

Forward kinematics is a commonly used method to determine the spatial position of the end-effector relative to a reference coordinate system. Denavit and Hartenberg [20] introduced a

systematic approach to this technique, which involves obtaining a homogeneous transformation matrix through a series of sequential transformations. These transformations include a d-translation along the z-axis, a θ-rotation about the z-axis, an a-translation along the x-axis, and an α-rotation about the x-axis, as expressed by Equations (1) and (2).

$$^{i-1}A_i = T_z(d)R_z(\theta)T_x(a)R_x(\alpha) \tag{1}$$

$$^{i-1}A_i = \begin{bmatrix} cos\,\theta_i & -cos\,\alpha_i\,sin\,\theta_i & sin\,\alpha_i\,sin\,\theta_i & a_i\,cos\,\theta_i \\ sin\,\theta_i & cos\,\alpha_i\,cos\,\theta_i & -sin\,\alpha_i\,cos\,\theta_i & a_i\,sin\,\theta_i \\ 0 & sin\,\alpha_i & cos\,\alpha_i & d_i \\ 0 & 0 & 0 & 1 \end{bmatrix} \tag{2}$$

Table 1 displays the Denavit-Hartenberg (D-H) parameters of the 3 degree-of-freedom (DOF) robot, which are utilized to characterize the kinematic interdependence between the robot's joints and end-effectors.

Table 1. Denavit-Hartenberg (D-H) Parameters of the 3 Degree-of-Freedom (DOF) Robot

i	$\boldsymbol{d}$ **[mm]**	$\boldsymbol{\theta}$ [°]	$\boldsymbol{a}$ **[mm]**	$\boldsymbol{\alpha}$[°]
1	d_1	0	0	$\pi/2$
2	0	L_2	0	0
3	0	L_3	0	0

In Equation (3), the center of mass for each body is explicitly defined with reference to its individual coordinate system.

$$\begin{aligned} ^1r_1 &= [0 \quad 0 \quad -d_1/2]^T \\ ^2r_2 &= [-L_2/2 \quad 0 \quad 0]^T \\ ^3r_3 &= [-L_3/2 \quad 0 \quad 0]^T \end{aligned} \tag{3}$$

As per the methodology explained in reference [21], the computation of actuator torque related to the i-th joint can be achieved through Equation (4). The acceleration-related symmetric matrix is described in Equation (5), and its characteristics have been elucidated in prior studies [20, 21]. τ_{ei} represents the impedance torque that acts on the i-th joint. The velocity matrix, denoted as U_{ij}, symbolizes the mathematical representation of the velocity of the i-th body concerning the j-th joint angle, conventionally indicated as θ_j. This matrix is defined using Equation (6), which presents a formal expression for the relationship between the velocity of the body and the joint angle.

$$M(q)\ddot{\theta}_\iota + C\left(\theta_i, \dot{\theta}_\iota\right) + G(\theta_i) = \tau_{act,i} + \tau_{ei} \tag{4}$$

$$M_{ik} = \sum_{j=max(i,k)}^{n} Tr\left(U_{jk}J_jU_{ji}^T\right) \tag{5}$$

$$U_{ij} = \begin{cases} ^0A_{j-1}\ Q\ ^{j-1}A_i & ,j \le i \\ 0 & ,j > i \end{cases} \tag{6}$$

The computation of the derivative of a homogeneous matrix ‘A’ can be achieved through left multiplication with the Q matrix, which represents the rotational component of the transformation matrix for revolute joints. The Q matrix is expressed by Equation (7), and its utilization is fundamental for obtaining the derivative of the homogeneous matrix A,

representing a pivotal step in the kinematic analysis of robotic systems.

$$Q = \begin{bmatrix} 0 & -1 & 0 & 0 \\ 1 & 0 & 0 & 0 \\ 0 & 0 & 0 & 0 \\ 0 & 0 & 0 & 0 \end{bmatrix} \tag{7}$$

In Equation (5), the trace operator, which calculates the sum of the diagonal elements of a matrix, is utilized as a mathematical tool commonly employed in linear algebra. This operator is designated by the symbol Tr and its definition has been established in prior works by Fu et al. [21] and Weisstein [22]. The precise definition of the trace operator is presented in Equation (8), which provides a succinct mathematical representation of the operator.

$$Tr(a) = \sum_{i=1}^{n} a_{ii} \tag{8}$$

The torques, τ_{act1}, τ_{act2}, and τ_{act3}, can be obtained by expanding the equation of motion represented by Equation (4). By expanding Equations (9) to (11), it is feasible to calculate the required torques needed to produce the observed motion of the system.

$$\begin{aligned} \tau_{act1} = & -\frac{1}{12}(12m_3 + m_1)L_2^2\dot{\theta}_1\dot{\theta}_2 sin(2\theta_2) - \frac{1}{12}(\dot{\theta}_2 + \dot{\theta}_3)L_3^2\dot{\theta}_1 m_2 sin(2\theta_2 + 2\theta_3) \\ & - \frac{1}{2}L_2L_3\dot{\theta}_1\dot{\theta}_3 m_3 sin(\theta_3) - \frac{1}{2}d_1 g m_1 sin(\theta_1) + \frac{1}{2}L_2L_3 cos(2\theta_2 + \theta_3)\dot{\theta}_6 m_3 \\ & + \frac{1}{24}((12m_3 + m_1)L_2^2 + (12m_3 + m_1)L_2^2 cos(2\theta_2) + 12L_2L_3 cos(\theta_3)m_3 \\ & + 24I_1 + L_3^2 m_2)\dot{\theta}_6 + \frac{1}{24}L_3^2 cos(2\theta_2 + 2\theta_3)\dot{\theta}_6 m_2 + \frac{1}{4}(2m_3 \\ & + m_2)L_2 cos(-\theta_2 + \theta_1)g + \frac{1}{4}(2m_3 + m_2)L_2 cos(\theta_1 + \theta_2)g + \frac{1}{4}L_3 cos(-\theta_2 \\ & - \theta_3 + \theta_1)g m_3 + \frac{1}{4}L_3 cos(\theta_1 + \theta_2 + \theta_3)g m_3 - (\frac{1}{2}\dot{\theta}_3 \\ & + \dot{\theta}_2)L_2L_3\dot{\theta}_1 m_3 sin(2\theta_2 + \theta_3) \end{aligned} \tag{9}$$

$$\tau_{act2} = -\frac{1}{2}L_2L_3\dot{\theta}_3^2m_3sin(\theta_3) - \frac{1}{4}((2m_3 + m_2)L_2 + L_3cos(\theta_3)m_3)cos(-\theta_2 + \theta_1)g - \frac{1}{4}L_3gm_3sin(-\theta_2 + \theta_1)sin(\theta_3) - \frac{1}{4}L_3gm_3sin(\theta_1 + \theta_2)sin(\theta_3) + \frac{1}{2}((\frac{1}{12}(12m_3 + m_1)L_2 + L_3cos(\theta_3)m_3)L_2 + \frac{1}{12}L_3^2cos(2\theta_3)m_2)\dot{\theta}_1^2sin(2\theta_2) + \frac{1}{2}(\frac{1}{12}L_3m_2sin(2\theta_3) + L_2m_3sin(\theta_3))L_3cos(2\theta_2)\dot{\theta}_1^2 + \frac{1}{24}((2m_1 + 24m_3)L_2^2 + 2L_3^2m_2 + 24L_2L_3cos(\theta_3)m_3)\dot{\theta}_5 + \frac{1}{24}(12L_2L_3cos(\theta_3)m_3 + 2L_3^2m_2)\dot{\theta}_4 + \frac{1}{4}((2m_3 + m_2)L_2 + L_3cos(\theta_3)m_3)cos(\theta_1 + \theta_2)g - L_2L_3\dot{\theta}_2\dot{\theta}_3m_3sin(\theta_3) \quad (10)$$

$$\tau_{act3} = -\frac{1}{4}L_3cos(-\theta_2 - \theta_3 + \theta_1)gm_3 + \frac{1}{12}L_3^2\dot{\theta}_4m_2 + \frac{1}{2}L_2L_3\dot{\theta}_2^2m_3sin(\theta_3) + \frac{1}{24}(12L_2L_3cos(\theta_3)m_3 + 2L_3^2m_2)\dot{\theta}_5 + \frac{1}{24}L_3^2\dot{\theta}_1^2m_2sin(2\theta_2 + 2\theta_3) + \frac{1}{4}L_2L_3\dot{\theta}_1^2m_3sin(2\theta_2 + \theta_3) + \frac{1}{4}L_2L_3\dot{\theta}_1^2m_3sin(\theta_3) + \frac{1}{4}L_3cos(\theta_1 + \theta_2 + \theta_3)gm_3 \quad (11)$$

3. IMPLEMENTATION OF IMPEDANCE CONTROL

The schematic representation of the impedance control methodology is presented in Figure 2. The implementation involves computing the forward kinematics and inverse dynamics equations to obtain the desired interaction point position of the robot, based on the joint angles. Any discrepancy between the derived position from forward kinematics and the target position is transformed into an interaction force through multiplication by the spring constant and damping coefficients. Subsequently, this force is multiplied by the transpose of the Jacobian matrix, which results in the generation of torques at the joints. These computed torques from inverse dynamics are then combined with the torques derived from the impedance control approach to obtain the final torque that is ultimately transmitted to the robot, thereby ensuring efficient control of the system.

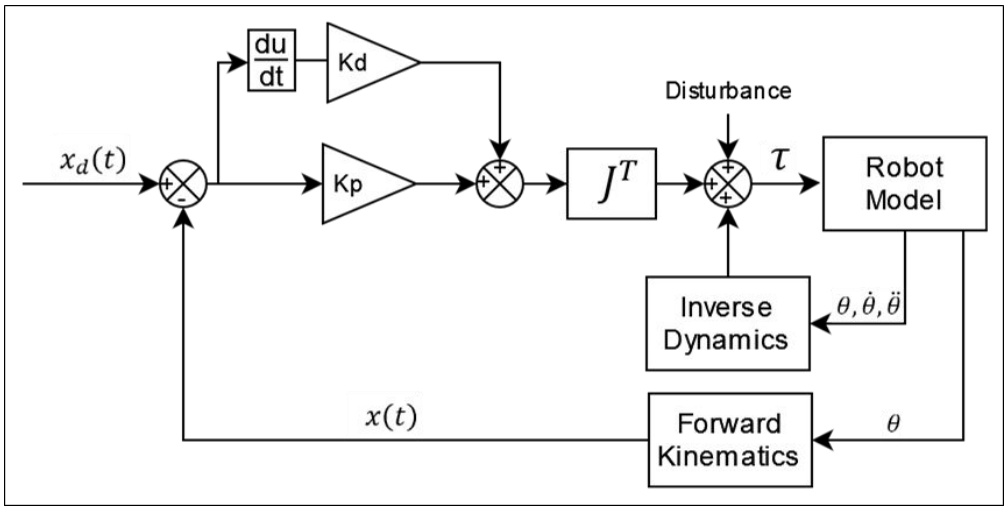

Figure 2. Schematic representation of the implementation of impedance control methodology for robotic systems

Equation (12) presents the mathematical expression for the interaction force produced by the Proportional-Integral-Derivative (PID) control method.

$$F_{int} = k\begin{bmatrix} x_{3d} - x_3 \\ y_{3d} - y_3 \\ z_{3d} - z_3 \end{bmatrix} + b\begin{bmatrix} \dot{x}_{3d} - \dot{x}_3 \\ \dot{y}_{3d} - \dot{y}_3 \\ \dot{z}_{3d} - \dot{z}_3 \end{bmatrix} + i\int \begin{bmatrix} x_{2d} - x_2 \\ y_{2d} - y_2 \\ z_{3d} - z_3 \end{bmatrix} dt \tag{12}$$

In this study, an impedance controller utilizing a PID control algorithm is employed to regulate the interaction force between the robot and the environment. The spring coefficient and damping coefficient of the impedance controller are designated as k and b, respectively, while the integral gain is represented by i. The target position of the robot's endpoint is defined as x_{3d}, y_{3d} and z_{3d} and is compared to the actual position of the endpoint, denoted as x_3, y_3 and z_3. The position of the robot's endpoint is mathematically expressed by Equation (13).

$$\begin{aligned} x_3 &= ((L_2 + L_3cos(\theta_3))cos(\theta_2) - L_3sin(\theta_2)sin(\theta_3))cos(\theta_1) \\ y_3 &= ((L_2 + L_3cos(\theta_3))cos(\theta_2) - L_3sin(\theta_2)sin(\theta_3))sin(\theta_1) \\ z_3 &= (L_2 + L_3cos(\theta_3))sin(\theta_2) + L_3cos(\theta_2)sin(\theta_3) + d_1 \end{aligned} \tag{13}$$

To convert the interaction force obtained from Equation (12) into torques, it is necessary to multiply it by the Jacobian matrix of the endpoint of the robot, which characterizes the relationship between the joint velocities and the endpoint velocity. The mathematical representation for the Jacobian matrix of the system is given in Equation (14).

$$J_f = \begin{bmatrix} \frac{dx_3}{d\theta_1} & \frac{dx_3}{d\theta_2} & \frac{dx_3}{d\theta_3} \\ \frac{dy_3}{d\theta_1} & \frac{dy_3}{d\theta_2} & \frac{dy_3}{d\theta_3} \\ \frac{dz_3}{d\theta_1} & \frac{dz_3}{d\theta_2} & \frac{dz_3}{d\theta_3} \end{bmatrix} = \begin{bmatrix} J_{f11} & J_{f12} & J_{f13} \\ J_{f21} & J_{f22} & J_{f23} \\ J_{f31} & J_{f32} & J_{f33} \end{bmatrix} \tag{14}$$

$$\begin{aligned} J_{f11} &= -((L_2 + L_3cos(\theta_3))cos(\theta_2) - L_3sin(\theta_2)sin(\theta_3))sin(\theta_1) \\ J_{f12} &= -((L_2 + L_3cos(\theta_3))sin(\theta_2) + L_3cos(\theta_2)sin(\theta_3))cos(\theta_1) \\ J_{f13} &= -(cos(\theta_2)sin(\theta_3) + cos(\theta_3)sin(\theta_2))L_3cos(\theta_1) \end{aligned}$$

$$J_{f21} = ((L_2 + L_3cos(\theta_3))cos(\theta_2) - L_3sin(\theta_2)sin(\theta_3))cos(\theta_1)$$
$$J_{f22} = -((L_2 + L_3cos(\theta_3))sin(\theta_2) + L_3cos(\theta_2)sin(\theta_3))sin(\theta_1)$$
$$J_{f23} = -(cos(\theta_2)sin(\theta_3) + cos(\theta_3)sin(\theta_2))L_3sin(\theta_1)$$
$$J_{f31} = 0$$
$$J_{f32} = (L_2 + L_3cos(\theta_3))cos(\theta_2) - L_3sin(\theta_2)sin(\theta_3)$$
$$J_{f33} = (-sin(\theta_2)sin(\theta_3) + cos(\theta_2)cos(\theta_3))L_3$$

The computation of impedance torques, τ_e, involves the multiplication of interaction forces by the transpose of the Jacobian matrix. This process is formalized mathematically in Equation (15).

$$\begin{aligned}
\tau_e &= J_f^T F_{int} \\
\tau_{e1} &= -((L_2 + L_3cos(\theta_3))cos(\theta_2) - L_3sin(\theta_2)sin(\theta_3))(-F_ycos(\theta_1) + F_xsin(\theta_1)) \\
\tau_{e2} &= (-(L_2 + L_3cos(\theta_3))F_xcos(\theta_1) - F_yL_2sin(\theta_1) - F_yL_3cos(\theta_3)sin(\theta_1) \\
&\quad - F_zL_3sin(\theta_3))sin(\theta_2) - (-F_zL_2 - F_zL_3cos(\theta_3) + F_xL_3cos(\theta_1)sin(\theta_3) \\
&\quad + F_yL_3sin(\theta_1)sin(\theta_3))cos(\theta_2) \\
\tau_{e3} &= -(((F_xcos(\theta_1) + F_ysin(\theta_1))cos(\theta_3) + F_zsin(\theta_3))sin(\theta_2) + ((F_xcos(\theta_1) \\
&\quad + F_ysin(\theta_1))sin(\theta_3) - F_zcos(\theta_3))cos(\theta_2))L_3
\end{aligned} \tag{15}$$

In Equation (15), the F_{int} force components along the x-axis and y-axis are denoted as F_x and F_y, respectively. The overall torques acting on the system are the summation of actuator torques and impedance torques obtained from Equation (8) and Equation (15).

4. NUMERICAL APPLICATION

The present study focuses on a robot system with specific physical parameters, such as $d_1 = 0.2625\ m$, $L_2 = L_3 = 1\ m$ and $m_1 = m_2 = m_3 = 5\ kg$. As per the provided scenario, the robot's endpoint sequentially moves from its initial position at point 1 to reach point 8 using ramp function, as depicted in Figure 3. The robot's endpoint exerts a steady force of 50 N on the plane defined by points 1, 2, 3, and 4.

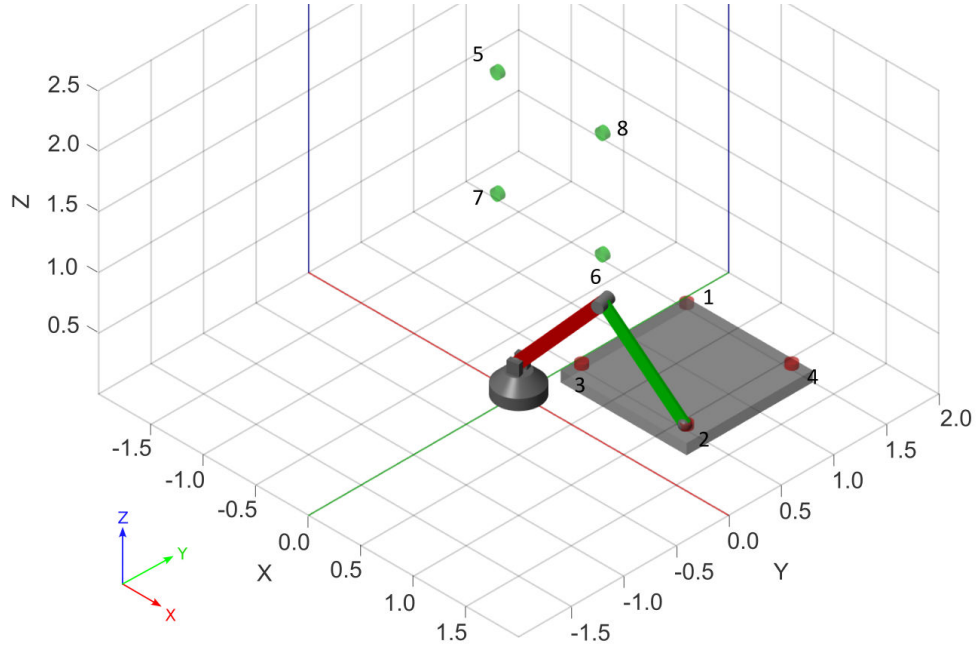

Figure 3. Numerical representation of the robot system and its motion trajectory

The desired point location from point 1 to point 8 is given in Table 2.

Table 2. Desired Point Locations.

Point No	X [m]	Y [m]	Z [m]	Point No	X [m]	Y [m]	Z [m]
1	0.3	1.3	0.25	5	-1.2	1	1.55
2	1.3	0.3	0.25	6	-0.2	1	0.55
3	0.3	0.3	0.25	7	-1.2	1	0.55
4	1.3	1.3	0.25	8	-0.2	1	1.55

To apply a consistent force of 50 N to the surface while the robot's tip point moves along the path from point 1 to point 4, we incorporate the 50 N force from the tip point to the ground into the interaction force specified in Equation (16).

$$F_{int,modified} = F_{int} + 50 \begin{bmatrix} 0 \\ 0 \\ -1 \end{bmatrix} \tag{16}$$

The optimization process for the coefficients k, b, and i in Equation (12) is guided by an objective function, which is mathematically expressed as Equation (17).

$$f_{obj} = \int_{t_1}^{t_2} (x_{3d} - x_3)^2 + (y_{3d} - y_3)^2 + (z_{3d} - z_3)^2 + (F_z - 50N)^2{}_{p1..4} \tag{17}$$

The optimization process of the coefficients k, b, and i in Equation (12) is performed by formulating an objective function that incorporates the square of the difference between the actual and target positions, commonly referred to as the distance error. Additionally, the objective function involves squaring the difference between the force applied by the endpoint and the surface formed by points 1 and 4, set to a constant value of 50 N. The aim is to minimize this objective function to reduce the distance error. The parameters used for The Bees Algorithm are specified in Table 3.

Table 3. The Bees Algorithm parameters

n	m	e	nep	nsp	ngh	p_{max}	p_{min}
10	7	4	5	3	0.1	[250,50,20]	[0,0,0]

3. RESULTS AND DISCUSSION

The outcomes of the PID-based impedance control parameters optimization via The Bees Algorithm are tabulated in Table 4. The optimization process encompassed 1000 iterations.

Table 4. The results of The Bees Algorithm

Initial Conditions			Initial Objective Function	The Bees Algorithm Result			Resulting Objective Function
k	b	i		k	b	i	
238.84	49.62	10.66	6602.60	79.17	32.41	6.65	3374.35

The convergence graph during the optimization of the objective function shown in Figure 4. The reaction force of the plate is shown in Figure 5. The force exhibits two peaks, measuring 54.01 N and 31.21 N, respectively. The final positions of the robot during the scenario are depicted in Figure 6.

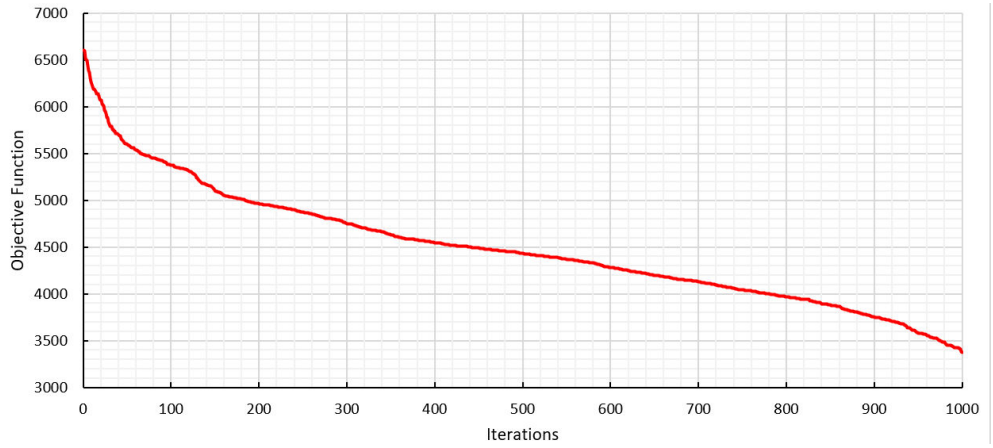

Figure 4. Convergence graph of the objective function.

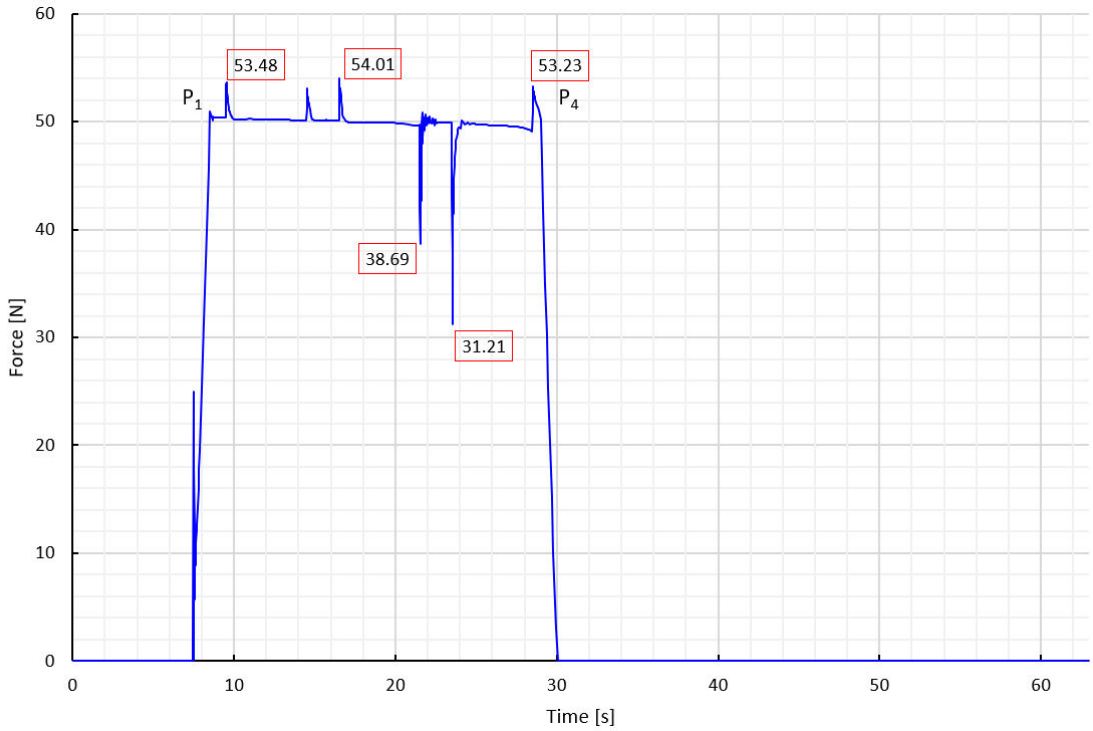

Figure 5. Reaction Force of the Plate

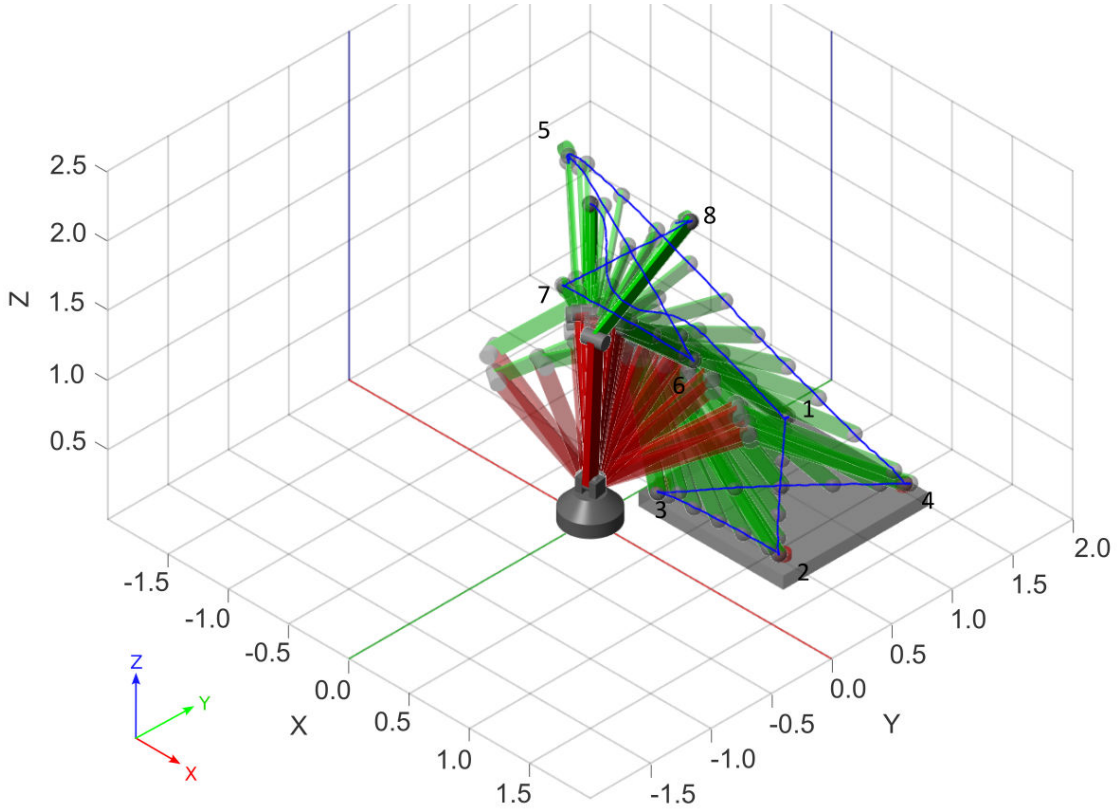

Figure 6. Movement of the robot's endpoint

CONCLUSIONS

In this study, the position of the endpoint of a 3 DOF robot was controlled using the impedance control technique. During the movement of the robot's endpoint on a plane, a change was made to the impedance force to apply a workload of 50 N. The applied workload exhibited peak errors of -37.5% and +8%. In addition, the impedance controller parameters were optimized using The Bees Algorithm. With an initial condition from a previous study, an improvement of 48.9% was achieved through optimization.

This study demonstrates that the impedance control technique can be used to apply a force in a desired direction while the endpoint of the robot moves along a trajectory. Future studies may consider exploring the use of this technique on surfaces other than a plane, such as in the polishing of surfaces. Overall, this research contributes to the development of advanced control techniques for robotic systems, with potential applications in various fields including manufacturing, healthcare, and beyond.

REFERENCES

[1] Bicchi, A., Kumar, V., 2000, *Robotic grasping and contact: A review*, Proc. Proceedings 2000 ICRA. Millennium conference. IEEE international conference on robotics and automation. Symposia proceedings (Cat. No. 00CH37065), IEEE, pp. 348-353.

[2] Pliego-Jiménez, J., Arteaga-Pérez, M. A., 2015, *Adaptive position/force control for robot manipulators in contact with a rigid surface with uncertain parameters,* European Journal of Control, 22(pp. 1-12.

[3] Hogan, N., 1984, *Impedance control: An approach to manipulation*, Proc. 1984 American control conference, IEEE, pp. 304-313.

[4] Hogan, N., 1984, *Impedance control of industrial robots,* Robotics and computer-integrated manufacturing, 1(1), pp. 97-113.

[5] Hogan, N., 1987, *Stable execution of contact tasks using impedance control*, Proc. Proceedings. 1987 IEEE International Conference on Robotics and Automation, IEEE, pp. 1047-1054.

[6] Erdemir, A., Kalyoncu, M., *Optimal Impedance Control of A 2R Planar Robot Manipulator*, in *Mas 17th International European Conference on Mathematics, Engineering, Natural & Medical Sciences*. 2023: Cairo, Egypt. p. 82-92.

[7] Wang, J., Li, Y., 2010, *Hybrid impedance control of a 3-DOF robotic arm used for rehabilitation treatment*, Proc. 2010 IEEE International Conference on Automation Science and Engineering, IEEE, pp. 768-773.

[8] Erdemir, A., Kalyoncu, M., *Modeling Impedance Control with Limited Interaction Power for A 2R Planar Robot Arm*, in *4th Latin American International Congress on Natural and Applied Sciences*. 2023: Rio de Janeiro, Brazil. p. 107-119.

[9] Erdemir, A., Kalyoncu, M., *Optimization of a Multi-Axle Steered Heavy Vehicle Steering Mechanism by using the Bees Algorithm and the Hooke-Jeeves Algorithms Simultaneously*, in *International Symposium on Automotive Science And Technology (ISASTECH 2019)*. 2019: Ankara/Turkey. p. 613-622.

[10] Lau, T. L., 1999, *Guided genetic algorithm,* pp. v, 166 leaves.

[11] Ortmann, M., Weber, W., 2001, *Multi-criterion optimization of robot trajectories with evolutionary strategies*, Proc. Proceedings of the 2001 Genetic and Evolutionary Computation Conference. Late-Breaking Papers, Morgan Kaufmann San Francisco, CA, pp. 310-316.

[12] Wang, D., Tan, D., Liu, L., 2018, *Particle swarm optimization algorithm: an overview,* Soft computing, 22(2), pp. 387-408.

[13] Pham, D., Kalyoncu, M., 2009, *Optimisation of a fuzzy logic controller for a flexible single-link robot arm using the Bees Algorithm*, Proc. 2009 7th IEEE International Conference on Industrial Informatics, IEEE, pp. 475-480.

[14] Erdemir, A., Kalyoncu, M., *Bir Ağır Vasıtanın Çok Akslı Direksiyon Mekanizmasının Arı Algoritması Kullanılarak Optimizasyonu*, in *Uluslararası Katılımlı 17. Makina Teorisi Sempozyumu UMTS 2015*. 2015. p. 421-426.

[15] Pham, D. T., Koç, E., Kalyoncu, M., Tınkır, M., *Hierarchical PID controller design for a flexible link robot manipulator using the bees algorithm*, in *Proceedings of 6th International Symposium on Intelligent Manufacturing Systems*. 2008. p. 757-765.

[16] Hooke, R., Jeeves, T. A., 1961, *``Direct Search''Solution of Numerical and Statistical Problems,* Journal of the ACM (JACM), 8(2), pp. 212-229.

[17] Ypma, T. J., 1995, *Historical development of the Newton–Raphson method,* SIAM review, 37(4), pp. 531-551.

[18] Erdemir, A., Kalyoncu, M., *Comparison of Energy Consumptions of Input Trajectory Functions in Impedance Controlled 2R Planar Robot Manipulator*, in *International Euroasia Congress on Scientific Researches and Recent Trends 10*. 2023: Baku, Azerbaijan. p. 312-325.

[19] Erdemir, A., Alver, V., Kalyoncu, M., *Arı Algoritması Kullanılarak Önden Dümenlemeli Bir Aracın Dümenleme Mekanizmasının Optimizasyonu*, in *International Aegean Conferences on Innovation Technologies & Engineering 6*. 2022: İzmir, Türkiye. p. 50-59.

[20] Denavit, J., Hartenberg, R., 1956, *Closure to" Discussions of'A Kinematic Notation for Lower-Pair Mechanisms Based on Matrices'"(1956, ASME J. Appl. Mech., 23, pp. 151–153),* Journal of Applied Mechanics, 23(1), pp. 153.

[21] Fu, K. S., Gonzalez, R., Lee, C. G., 1987, *'Robotics: Control, Sensing, Vision, and Intelligence'*, Tata McGraw-Hill Education, 580 p.

[22] Weisstein, E. W., 2002, *CRC concise encyclopedia of mathematics*, Chapman and Hall/CRC, 1984 p.